High magnetic moment CoFe nanoparticles

L. Bessais[1], K. Zehani[1], R. Bez[1,4], J. Moscovici[1], H. Lassri[2], E. K. Hlil[3] and N. Mliki[4]

[1]CMTR, ICMPE, UMR7182, CNRS-UPEC, 2 rue Henri Dunant F-94320 Thiais, France
[2]LPMMAT, Université Hassan II, Faculté des Sciences Ain Chock, Casablanca, Maroc
[3]Institut Néel, CNRS et Université Joseph Fourier, F-38042 Grenoble cedex 9, France
[4]LMOP, Faculté des Sciences de Tunis, Campus Universitaire, 2092 Tunis, Tunisia

Keywords: Transition metal alloys, Magnetic properties, HRTEM.

Abstract

A new way of preparing CoFe nanoparticles has been developed using the polyol reduction process followed by heat treatment under argon. The atomic ratio of Co/Fe was set to be 45:55. All the synthesized samples of CoFe nanoparticles were annealed at 600°C for different annealing times. The structure properties of these compounds have been characterized by X-ray diffraction and analyzed using the Rietveld refinement method. Body-centered-cubic phase structure was observed for all annealed samples and increased with annealing time up to 99 wt.%. The magnetic characterization of the samples, after and before annealing, were measured using a Physical Properties Measurement System. The magnetic properties are improved with annealing time, and the best results were obtained for 4h. The coercivity is equal to 112 Oe and saturation magnetization reaches 235 emu/g.

Introduction

Nanocrystalline ferromagnetic materials exhibit interesting magnetic properties from the point of view of fundamental research up to applications. These materials have taken a privileged place in the research of new soft magnetic materials [1]. Recently, several researches have been made on the study of the FeCo soft magnetic nanomaterials [2]. These materials are interesting for various applications. Because of their unique magnetic properties (high saturation magnetization, large permeability, low coercivity and ferromagnetic behavior up to 1073 K), they are used in transformer cores, electrical generators, electrical motors, pole pieces and for hyperthermia-based therapy [3]. The optimization of the structure and microstructure represents the key of success to develop the magnetic properties of these samples. They may be synthesized by high energy milling or chemical route [4].
N. Poudyal et al. have prepared FeCo nanomaterials by surfactants-assisted ball milling; they have found that saturation magnetization of FeCo (obtained by ball milling for 1h) is 209 $Am^2.kg^{-1}$ with 23 nm of nanoparticles size [4]. M. Zamanpour et al. were able to synthesize nanoparticles FeCo by polyol using ethylene glycol (EG) as solvent; they obtained a saturation magnetization of 200 $Am^2.kg^{-1}$ for nanoparticles size of 30 nm [5].

In this paper, we present high magnetic moment $Fe_{1-x}Co_x$ (x = 0.45) nanoparticles synthesized by a novel route - the polyol process - followed with annealing under argon. We have carried out structural investigation by careful powder X-ray diffraction (XRD)

analysis with Rietveld refinements [6], transmision electron microscopy coupled with energy dispersive spectroscopy (EDS) analysis, and measurement hysteresis loop. In addition to the experiments, the Magnetic Anisotropy (MA) was estimated using random anisotropy approach.

Experimental Methods

The powders of $Fe_{55}Co_{45}$ nanoparticles were synthesized by reduction polyol method [7]. High purity analytical grade cobalt acetate anhydrous ($Co(Ac)_2$), iron chloride tertra hydrate ($FeCl_2.4H_2O$), diethylene glycol (DEG), sodium hydroxide (NaOH) and ruthenium chloride ($Ru(Cl_2)$) were used in synthetic reaction without any further treatment. The first step of the synthesis of metal nanoparticles is to process spinels $CoFe_2O_4$ nanoparticles via forced hydrolysis in a polyol medium [8]. The second step is to reduce them by argon gas at 873 K. $CoFe_2O_4$ was synthesized, starting from an amount precursor salts of 100 mmol of $FeCl_2.4\ H_2O$ and 80 mmol of cobalt acetate $Co(CH_3COO)_2.4\ H_2O$. The acetate ratio defined as $\frac{[M]}{[OAs]}$ (M stands for the total amount of metallic elements), was fixed to 2.2. The total volume of the DEG is 200 ml. We have dissolved also 5 mmol of ruthenium chloride and 1.26 M of sodium hydroxide. The mixture was then heated at 418 K for 2h with a rate of 5 $K.min^{-1}$. After completion of the reaction the produced powder was filtered, washed with ethanol and acetone, and dried at 353 K.
After polyol synthesis, the nanopowder wrapped in tantalum foils were annealed in a sealed silica tube under 10^{-6} Torr at 873 K during 30 min, 1, 2, and 4 hours.
The structural properties of the samples obtained before and after annealing were characterized by the powder X-ray diffraction using the BRUKER diffractometer with Cu K_α target ($\lambda = 1.5406\mathring{A}$) to determine the crystallographic structure and to identify phases. The intensities were measured at angles from $2\theta = 20°$ to $90°$ with a step size $0.02°$. The structure refinement for the X-ray pattern was carried out using MAUD computer code based on Rietveld analysis [6]. Transmission Electron microscopy (TEM), high resolution transmission electron microscopy (HRTEM) and selected area electron diffraction (SAED) were performed using a JEOL 2010 FEG microscope operating at 200 kV. The chemical composition of the grains was determined by energy dispersive spectroscopy. The magnetic measurements of the samples were measured using a Physical Properties Measurement System (PPMS9 Quantum Design) under an applied field up to 3T.

Results and Discussions

Structure analysis

The annealing of the polyol powders is accompanied by a decrease of the XRD intensities of Co ferrite peaks and the apparition of FeCo peaks. The peaks of $CoFe_2O_4$ are due to the oxidation of Fe^{2+} to Fe^{3+} during reaction which combines with Co^{2+} to form Co ferrite. Cobalt ferrite phase is observed no more in samples annealed for 4h.

Figure 1 presents, as an example the Rietveld analysis results of XRD pattern of FeCo sample after annealing for 4h at 873 K. The refinement performed for the as-synthesized sample shows the presence of a main phase of $CoFe_2O_4$ with spinel structure (space group

Fd-3m). The unit cell parameter a is equal to 8.4087 Å. (see Table 1)
Three characteristic peaks of FeCo phase corresponding to the crystal planes of (110), (200) and (211) were observed for all annealed and milled samples. The relative contribution of the two crystalline phases given by the Rietveld analysis varies with annealing time for a given temperature 873 K. With increasing the duration of annealing, the proportion of $Fe_{55}Co_{45}$ phase increases from 64.28% to 98.89% for 30 min and 4h respectively. After an annealing during 4h the structure refinement shows a main phase of

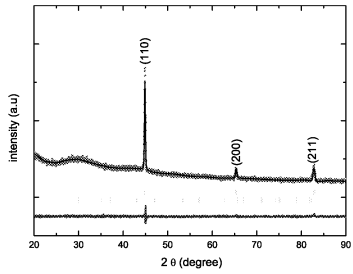

Figure 1: Rietveld analysis for X-ray diffraction pattern of FeCo as-synthesized (above) and annealed at 873 K for 4h (below)

$Fe_{55}Co_{45}$ with body centered cubic structure (bcc). The lattice parameter is $a = 2.8539$ Å. No additionnals peaks such as $Co(OH)_2$, $Fe(OH)_2$, are observed in XRD pattern which indicates the high purity of prepared sample. These results provide that increasing the annealing time is important for co-reduction of metal ions (Co^{2+} and Fe^{3+}) and favors the formation of alloy phase. The experimental conditions and structural characterization for all samples are summarized in Table 1.
The grain size and the strain of the nanoparticules was calculated using the Williamson-Hall equation [9]. The Williamson-Hall analysis shows an increase in the size of the FeCo nanoparticles and the strain with increase of annealing time from 30 min to 4h (Table 1).

Microstructural analysis

The size, the morphology of as-prepared product as well as these annealed during 4h were further examined by TEM, HREM and SAED. TEM Image shown in Fig. 2 indicated that the as-synthesized $CoFe_2O_4$ are composed of sphere-like nanoparticles well dispersed with diameters ranging between 5 and 12 nm (see size distribution in inset).

Fig.3a shows that after annealing for 4h at 873 K, the particle size is increased, and the crystallintiy is improuved. In Fig. 3b, we can see microdiffraction patterns obtained from the FeCo sample annealed for 4h at 873K. The diffracting crystal has its [100] axis parallel to the electronic beam. All patterns can be completely indexed with a

Table 1: Structural results of cobalt ferrite and FeCo samlpes, a is the unit cell parameter, wt.% is the phase abundance, the grain size D, and the strain ϵ are deduced from Williamson Hall analysis. The sample correspandes respectively to ferrite de cobalt and annealed at 873 K for an annealig duration of 30 min, 1h, 2h and 4h.

Sample	Phase	wt.%	a(Å)	D(nm)	ϵ
Cobalt ferrite	$Fe_{55}Co_{45}$	0.28	-	-	-
	$CoFe_2O_4$	99.72	8.4087(4)	10	
FeCo (30 min)	$Fe_{55}Co_{45}$	64.28	2.8460(3)	14	0.054
	$CoFe_2O_4$	35.72	8.3919(6)		
FeCo (1h)	$Fe_{55}Co_{45}$	77.22	2.8489(5)	16	0.063
	$CoFe_2O_4$	23.78	8.3948(2)		
FeCo (2h)	$Fe_{55}Co_{45}$	81.12	2.8512(6)	23	0.096
	$CoFe_2O_4$	18.88	8.3952(2)		
FeCo (4h)	$Fe_{55}Co_{45}$	98.89	2.8539(6)	66	0.135
	$CoFe_2O_4$	1.11	-	-	-

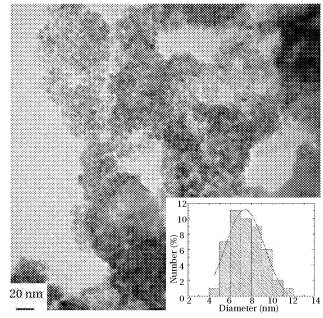

Figure 2: HRTEM images of cobalt ferrite.

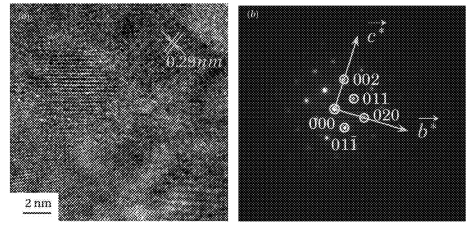

Figure 3: HRTEM (a), and Electron microdiffractions along [100] axis (b) of FeCo nanoparticles annealed for 4 h at 873 K.

body-centered cubic lattice and a unit cell parameter as determined from X-ray powder diffraction.

Magnetic measurements

The magnetic behavior of the $CoFe_2O_4$ ferrite particles varies with different Co^{2+} occupations since the Co^{2+} ion is highly anisotropic. To investigate the magnetic properties of the synthesized $CoFe_2O_4$ ferrite particles in polyol medium, the applied magnetic field dependence of magnetization M(H) are measured at room temperature, RT, (300 K, Fig.4) and low temperature, LT, (10 K, Fig.4).

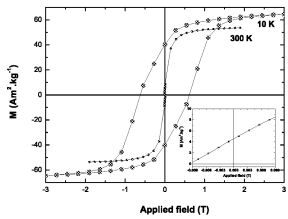

Figure 4: Hysteresis loops of the cobalt ferrite at 10 K and 300 K.

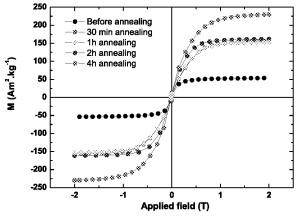

Figure 5: Hysteresis loops, at 300 K, for the cobalt ferrite before and after annealing for different times.

The hysteresis loops at 300 K shows a typical soft materials, with coercivity H_C of 0.22 mT, and saturation magnetization, M_S, of 55 $Am^2.kg^{-1}$. M_S were estimated from a fit over the high-field data using the approach to saturation magnetization law (see equation (1)). These values of the coercivity and the saturation magnetization are similar to the ones measured by Zhang et al. [10], for cobalt ferrite synthesized by hydrothermal process where they found $H_C = 0.37$ mT and $M_s = 52$ $Am^2.kg^{-1}$. The remanance magnetization value of M_r is equal to 4.94 $Am^2.kg^{-1}$ is obtained for cobalt ferrite (see Fig.4 inset). For nanosized ferrite particles (D = 10 nm), the surface area are larger; thus the surface energy and surface tension are high. This leads to changes in cationic preferences and thus lesser magnetizations [11]. In addition, there is a problem of superparamagnetic relaxation because for small particles the Néel's relaxation is dominant [12, 13].

At 10 K, a large hysteresis loops is obtained, showing hard magnetic behavior with coercive field H_c of 7.73 mT, as a result of blocking of the Néel relaxation. This confirms that most of particles as superparamagnetic at RT due to their small size. Remanance M_r of 40 $Am^2.kg^{-1}$, and saturation magnetization, M_s, of 65 $Am^2.kg^{-1}$ are observed leading to a squareness ratio, M_r/M_s of 0.62. This result can be discussed by considering an assembly of single domain particles with randomly oriented easy axis where H_c is expected to be proportional to K/M_s ratio, and $M_r/M_s = 0.5$ for axial anisotropy or $M_r/M_s = 0.85$ for the cubic anisotropy.

The magnetic properties of the powders synthesized are highly influenced by annealing time through formation of metallic FeCo and grain size increase. Hence, as can be seen in figure 5 and table 2, the structural and magnetic data exhibit a clear correlation. Figure 5 depicts the RT hysteresis loop of Co ferrite and $Fe_{55}Co_{45}$ after annealing under argon. The saturation magnetization at RT for the sample annealed during 4h is 235 $Am^2.kg^{-1}$, which is very close to the bulk value (237 $Am^2.kg^{-1}$) and slightly more than that obtained by polyol process (200 $Am^2.kg^{-1}$ with ethylen glycol as a solvent) [14].

This confirms the results obtained by X-ray diffraction, i.e. the formation of bcc FeCo phase. We can notice that M_r also increases with annealing time and the wt.% of FeCo, which is related to grain size increase that reduces the relaxation time.
To get insight the effect of annealing on the magnetic properties, we have tried to evaluate the magnetic anisotropy constant.

Random magnetic anisotropy constant

Table 2: Some magnetic parameters of the cobalt ferrite synthesized by polyol process before and after annealing for different times at 300 K.

Sample	M_s ($emu.g^{-1}$)	M_s (μ_B)	M_r ($emu.g^{-1}$)	H_c (Oe)	H_r (kOe)	K_L ($10^6 erg.cm^{-3}$)
FeCo as synthesized	55	2.27	4.94	173	1.2	0.18
FeCo (30 min)	159	1.62	4.16	129	0.81	0.53
FeCo (1h)	156	1.60	5.89	102	0.84	0.54
FeCo (2h)	164	1.68	6.72	82	0.90	0.60
FeCo (4h)	235	2.40	8.19	76	0.95	0.92

Random magnetic anisotropy (RMA) was first proposed by Harris and Plischke [15] to explain the anisotropy found in some amorphous alloys and particularly those containing rare earth metals. Based on their Hamiltonian, Chudnovsky [16] proposed a model to analyze the approach to saturation. This model was applied successfully to explain the results by several authors. We had used this model to analyse our results on several rare earth based amorphous alloys and obtained various fundamental parameters such as local anisotropy, the correlation lengths, etc. [17]. We propose to apply similar ideas to the nanomaterials. The application of this random anisotropy model to nanomaterials could be justified as follows. The nanograins due to their low dimension have a lower symmetry in the regions particularly near the surface, resulting in a kind of uniaxial anisotropy. As the grains are oriented at random there is no alignment of this axis which then leads to a spread in their direction. This is then analogous to the amorphous materials where the topological disorder leads to a spread in the axis of symmetry. The essential difference of course is that in the amorphous alloys the structural correlation length is of the order of 1 or 2 nm whereas in nonomaterials the grains size is an order of magnitude bigger. This would result in some differences in details and could affect the magnitude of the anisotropy. We briefly describe below the model we have used. We can describe the

approach to magnetic saturation by the formula [17]:

$$M(H) = M_s \left[1 - \frac{a_2}{(H+H_U+H_{ex})^2}\right] \qquad \text{with} \qquad a_2 = \frac{H_r^2}{15} = \frac{1}{15}\left(\frac{2K_L}{M_s}\right)^2 \tag{1}$$

where H is the applied magnetic field in (kOe), M_s is the saturation magnetization in (emu.g^{-1}), H_U is the coherent anisotropy field, H_{ex} is the exchange field, H_r is the random magnetic field, and a_2 is a constant which is a function of K_L the local anisotropy and M_s.

The magnetization curves for all samples are found to fit well equation (1) as shown in Fig.6. The values of M_s, and a_2 obtained from the fitting at 300K were used to determine K_L using Eq. (1). Values of the parameters obtained by this way are displayed on Table 2. We find that the local anisotropy increases from 0.18×10^6 erg.cm^{-3} to 0.92×10^6 erg.cm^{-3} before and after annealing for different times at 300 K.

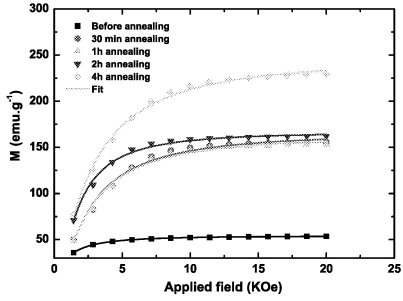

Figure 6: Magnetization curve of the cobalt ferrite synthesized by polyol process before and after annealing for different times at 300 K.

Conclusion

Polyol medium process followed annealing under argon has demonstrated to be an effective way. It has enabled us to develop a high magnetic moment for the $Fe_{55}Co_{45}$ nanoparticles. The Rietveld analysis for X-ray diffraction pattern, as well as TEM study, of samples annealed at different times showed an increased of the wt.% of FeCo nanoparticles (bcc structure) up to 99 % for annealing of 4h. The magnetic measurements have shown a high magnetization saturation (235 Am^2.kg^{-1}) and a low coercive field (7.5 mT). We have shown that it is possible to extend the application of random magnetic anisotropy model originally developed for amorphous alloys to the nanocrystalline materials of cobalt ferrite and FeCo alloys. The model gives a good fit of the experimental M(H). In addition, we have determined some fundamental parameters such as random anisotropy fields and random anisotropy constant. We found that the local anisotropy

is at least an order of magnitude higher than in the corresponding bulk FeCo alloys. Moreover, substantial interstitial magnetism is revealed in $CoFe_2O_4$ compound.

References

[1] M. E. McHenry, D. E. Laughlin, Acta Mater, 48, 223-238, **2000**.

[2] M. Y. Rafique, L. Pan, M. Z. Iqbal, Q. Javed, H. Qiu, R. U.Din, M.H. Farooq, Z. Guo, Journal of Alloys and Compounds, 550, 423430, **2013**.

[3] M. E. McHenry, M. A. Willard, D. E. Laughlin, Progress in Materials Science, 44, 291-433, **1999**.

[4] N. Poudyal, C. Rong, and J. Ping Liu, J. Appl. Phys. 109, 07B526, **2011**.

[5] M. Zamanpour, Y. Chen, B. Hu, K. Carroll, Z. J. Huba et al., J. Appl. Phys., 111, 07B528, **2012**.

[6] H. M. Rietveld, J. Appl.Crystallogr, 2, 65, **1969**.

[7] M. Abbas, M. N. Islam, B. P. Rao, T. Ogawa, M. Takahashi, C. Kim, Materials Letters, 91, 326-329, **2013**.

[8] U. Acevedo, T. Gaudisson, R. O. Zempoalteca, S. Nowak, S. Ammar et al., J. Appl. Phys. 113, 17B519, **2013**.

[9] A. K. Zak, W. H. Abd. Majid, M. E. Abrishami, R. Yousefi, Solid State Sciences, 13, 251-256, **2011**.

[10] Y. Zhang, Y. Liu, C. Fei, Z. Yang, Z. Lu et al., J. Appl. Phys. 108, 084312, **2010**.

[11] D. J. Fatemi, V. G. Harris, V. M. Browning, and J. P. Kirkland, J. Appl. Phys. 83, 6867, **1998**.

[12] J. L. Dormann, L. Bessais and D. Fiorani, Journal of Physics C-Solid State Physics, 21, 2015, **1988**.

[13] L. Bessais, L. BenJaffel and J. Dormann, Phys. Rev. B, 45, 7805-7815, **1992**,

[14] P. Weiss and R. Forrer, Ann. Phys. 12, 279, **1929**.

[15] R. Harris, M. Plichke, M. J. Zuckerman, Phys. Rev. Lett., 31, 160, **1973**.

[16] E. M. Chudnovsky and R. A. Serota, J. Phys. C, 16, 4181, **1983**.

[17] H. Lassri, R. Krishnan, J. Magn. Magn. Mater., 104-107, 157, **1992**.